Available online at www.sciencedirect.com
ScienceDirect
International Journal of Heat and Mass Transfer 50 (2007) 4503–4507
International Journal of HEAT and MASS TRANSFER
www.elsevier.com/locate/ijhmt

Technical Note

An experimental investigation on capillary pumped loop with the meshes wick

Jianlin Yu *, Hua Chen, Hua Zhao, Yanzhong Li

Department of Refrigeration and Cryogenic Engineering, School of Energy and Power Engineering, Xi'an Jiaotong University, Xi'an 710049, China

Received 19 June 2006; received in revised form 21 February 2007
Available online 2 May 2007

Abstract

A copper-water capillary pumped loop (CPL) is developed for heat recovery applications in the field of the refrigeration and air conditioning. The multi-layer copper meshes are used as the capillary structure in the CPL. The startup characteristics and heat transfer performance of the CPL are investigated experimentally. The experimental results show that for a range of power applied to the evaporator, the system presented reliable startups and continuous operation. The heat transfer performance of the evaporator will be improved if the charging rate of the working fluid or the heat flux is increased properly. The optimal charging rate could be obtained in the range of 70–76% for the given experimental conditions. The study has demonstrated the proposed CPL configuration is able to perform the heat recovery applications.
© 2007 Elsevier Ltd. All rights reserved.

Keywords: Capillary pumped loop; Heat transfer; Heat recovery

1. Introduction

The capillary pumped loop (CPL) uses the same basic principle as widely known heat pipe, i.e., closed evaporation–condensation cycle maintained by capillary pumping. The separation of the liquid and vapor transport lines is a key character of a CPL over a heat pipe. Thus, the major advantage of CPL over a heat pipe is that it can transport energy over a longer distance. CPL technology has been developed as an option for transporting thermal energy within spacecrafts, satellites and electronic components [1,2]. Moreover, numerous investigations have also been performed with the innovating CPL technology in the past. Muraoka et al. [3] investigated a new CPL with a condenser containing a porous wick structure. Bazzo and Nogoseke [4] proposed the capillary pumping system assisting flat solar collectors, which using fine circumferential grooves as capillary structure and acetone as the working fluid. A series of study on the thermal transport characteristics were also conducted on CPL systems. LaClair and Mudawa [5] developed an analytical model of conduction during the initial heating of a cylindrical capillary evaporator, which is applicable to standard CPL evaporators. Chen and Lin [6] investigated the effects of parameters on the CPL used for cooling of electronic components. Bazzo and Riehl [7] studied the operation characteristics of a small-scale capillary pumped loop. Pouzet et al. [8] studied the dynamic response of a capillary pumped loop subjected to various heat load transients.

Recently, there are efforts to extend the application of CPL to commercial and industrial systems. The use of such devices offers many advantages regarding the flexibility in operation and application, as they are very efficient in transporting heat, even under a small temperature difference. Therefore, CPL could also be used as heat recovery devices applied to the field of the refrigeration and air conditioning. For this purpose, this paper presents a novel design of a CPL, which uses multi-layer copper meshes as

* Corresponding author. Tel.: +86 29 82668738; fax: +86 29 82668725.
E-mail address: yujl@mail.xjtu.edu.cn (J. Yu).

0017-9310/$ - see front matter © 2007 Elsevier Ltd. All rights reserved.
doi:10.1016/j.ijheatmasstransfer.2007.02.038

the capillary structure in the evaporator. The startup characteristics of the CPL are investigated experimentally. The effects of the working fluid charging rate on the CPL operation are also investigated. Details of the CPL, test setup and test procedure are described in the following sections.

2. Description of CPL and experimental setup

The CPL configuration studied in this paper is schematically presented in Fig. 1. It is composed of an evaporator, condenser, liquid and vapor lines and a two-phase reservoir. The helical coiled condenser is made of a long copper pipe with the length of 0.8 m and the outer diameter of 8 mm. The two transport lines for vapor-phase and liquid-phase are thin-walled copper pipes with the inner diameter of 4 mm and the thermal transport distance is about 1.1 m. The reservoir is connected to the condenser through a copper pipe with the inner diameter of 4 mm, which is responsible for establishing the loop operation pressure and temperature, as well as the working fluid inventory in the CPL. In contrast with the conventional CPL configuration, in the present design the evaporator is equipped with a multi-layer copper mesh wick structure. Metal meshes, as tested here, are widely used as the capillary porous media in heat pipe wicks due to their low cost and relative simplicity of manufacture. Fig. 2 shows the schematic diagram of the evaporator. And some configuration parameters are listed in Table 1.

Distilled water is used as the working fluid in the present study. The working fluid must operate without impurities as an important condition. The presence of non-condensable gases (NCG) in a CPL can cause a general failure of the capillary evaporator. The presence of NCG in present CPL can be minimized because the materials in CPL are compatible with the selected working fluid. Moreover, to further avoid the presence of NCG in the loop, strict cleaning is carried out by using acetone solvent, mixed solution (the proportion of phosphorus acid and nitric acid is 1:1) and distilled water in procedure.

A charging system is also designed in order to ensure that the correct amount of water was charged into the loop. In this system, a vacuum-pump is connected to the CPL and the charging reservoir including a burette and a flask. The whole system is evacuated for a minimum of 8 h prior to charging. Distilled water is refluxed (boiled and condensed) in a flask to remove air. Charging is accomplished by operating the on/off of several vacuum valves from the vacuum-pump to the reservoir and loop system. The amount of fluid that is added to the CPL is controlled at the burette by keeping a meniscus in the graduated portion.

The experimental setup comprises heating system, cooling system and measurement system. Electrical resistance heaters are located on both the reservoir and evaporator as shown in Fig. 1. The wires, as a heater, are wound around the outer wall of the evaporator and the reservoir with a proportional interval for supplying the constant thermal load. The reservoir heater is connected to temperature controllers to maintain the temperature of the reservoir at the desired set point. On/off temperature controllers are used to control the reservoir heater. The condenser of CPL is cooled by the water tank with circulating water. In addition, the entire CPL except the condenser is insulated with thermal insulating material. The experiment data are collected by Agilent data acquisition system, model 34970A.

The temperatures along the CPL are measured with T-type thermocouples. The thermocouple locations are also shown in Fig. 1. All thermocouples were calibrated in conjunction with the data acquisition system. The accuracy of temperature measurement was at range of ±0.5 °C. The heater power of evaporator was calculated by multiplying the voltage and the current measured from the digital mul-

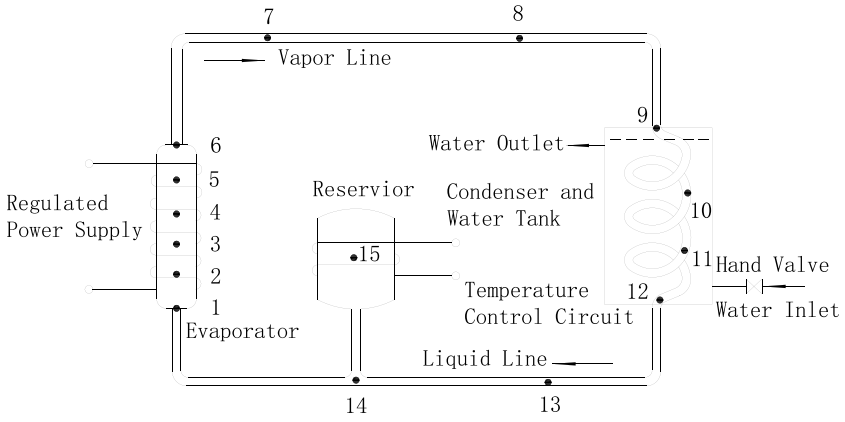

Point 1~ point 15 are points for measuring temperature.

Fig. 1. Schematic diagram of the experimental setup.

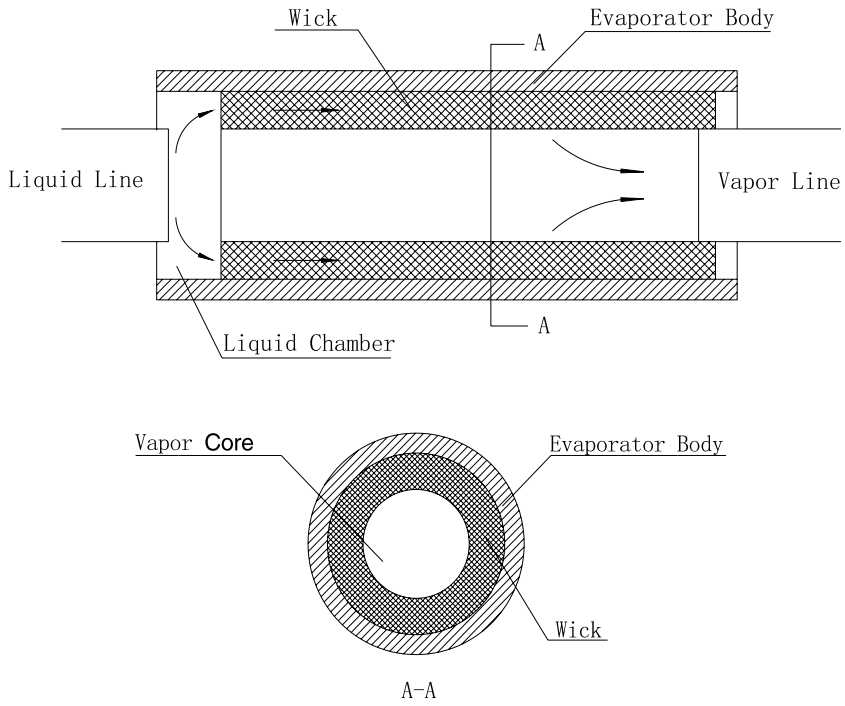

Fig. 2. Schematic diagram of the evaporator.

Table 1
Geometric characteristics of the evaporator

Wick		Evaporator body	
Length (mm)	190	Length (mm)	200
Outer diameter (mm)	10	Outer diameter (mm)	12
Inner diameter (mm)	6	Wall thickness (mm)	1
Material	Copper mesh	Material	Red copper
Parameter of mesh	400/cm^2, 8 layers	Working fluid	Distilled water

timeter. The error in the measurement of heater power is at range of 0.05 V for voltage and 0.01 A for current. The heat loss was estimated to be approximately 6% or less based on the insulation conductivity and thickness. The overall measurement uncertainty of the heat rate through the evaporator is predicted at about 4%. The maximum uncertainty in the heat transfer coefficient was 9%.

The experimental test is performed to investigate the thermal performance of the CPL. All test is carried out at the room temperature about 25 °C. In the following test, the working fluid charging rate is considered for variable case. The charging rate is defined as the ratio of the volume of working fluid charged and the total volume of the CPL. The calculation equation is as follows:

$$R = V_{\mathrm{wf}}/V_{\mathrm{cpl}} \tag{1}$$

where R is the charging rate, V_{wf} is the volume of working fluid and V_{cpl} is the total volume of the CPL.

3. Experiment results and discussion

3.1. Startup of the CPL

The CPL startup tests are the most critical for evaluating the capillary evaporator reliability. The following results are obtained when the reservoir temperature is 40 °C, heater power of evaporator is 20 W and 10 W, the charging rate is 75%. Fig. 3 shows the startup results for the heat load applied to the evaporator. It can be observed that after the evaporator heater is turned on, there is an increase in the temperature of the evaporator body (corresponding to the average temperature of point 2 to point 5), evaporator liquid inlet (point 1), and evaporator vapor exit (point 6) to the vapor line. The liquid inlet and vapor exit temperatures increase due to conductive heat leak from the evaporator body; the slope of the temperature traces for these locations is significantly smaller than the rate of rise of the evaporator body.

The startup time for low heat loads is longer than that for high heat loads. As seen in Fig. 3, at low heat loads (10 W), the startup time takes about 10 min to occur, while at high heat loads (20 W) the startup time takes about 4 min. It is possible that at low heat loads, the menisci formation in the wick take more time as heat is slowly transferred to the working fluid, causing a longer time to start generating capillary forces. At high heat loads, the menisci forms more quickly and the capillary forces begin to act faster. In general, the CPL has showed very fast response to the heat load applied to the capillary evaporator in order to efficiently perform the heat transport.

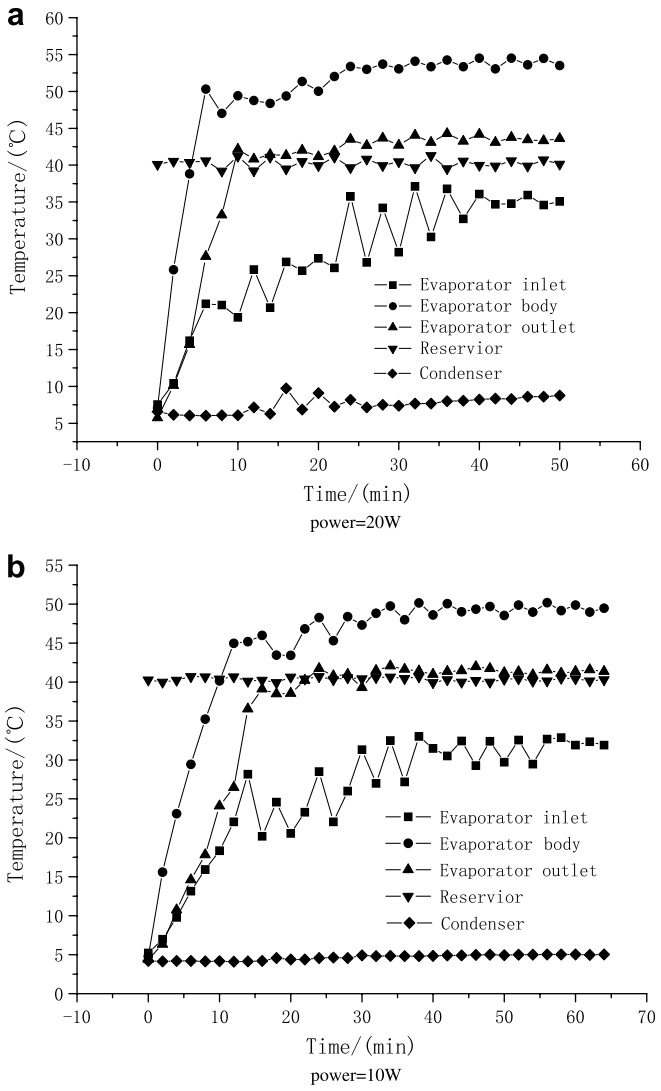

Fig. 3. Temperature change curve of the CPL in the startup process.

The steady state is achieved, at both low and high heat loads, in less than 25 min while the CPL operation remained very stable during the time. From the experimental tests, it is possible to verify that the CPL design give a reliable startups and continuous operation.

3.2. Heat transfer performance

At the end of startup, steady operations are observed from the change of wall temperatures of the outside evaporator body for all tests. Fig. 4 shows the distribution of wall temperatures of the outside evaporator body at different thermocouples positions with variation of the measuring time, at reservoir temperature is 40 °C, heater power 20 W and the charging rate 84%.

As shown in Fig. 4, the wall temperatures take on distinctive fluctuation with the rise of the thermocouples positions. The wall temperature at the position close the evaporator body exit was higher than that at the position near by inlet. However, it is found the temperature difference along the evaporator body is kept a constant during test. This implies that there is no change in evaporator conductance and steady state operation was reached.

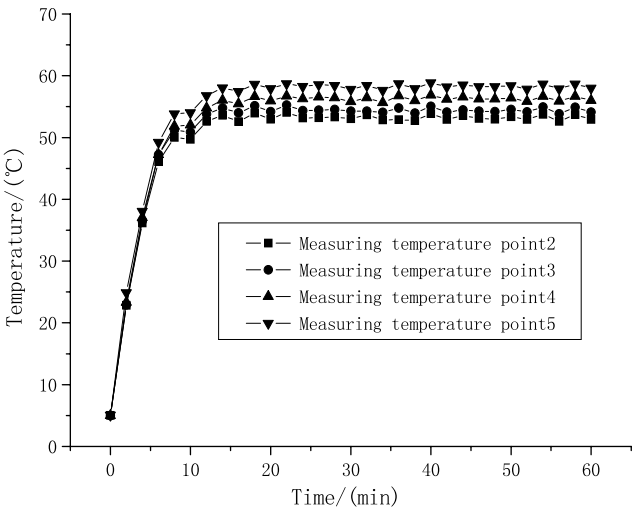

Fig. 4. Temperature curve for four points temperature of the evaporator body.

For studying heat transfer performance of the evaporator, the mean heat transfer coefficient h is defined as

$$h = q_e/\Delta t \tag{2}$$

$$q_e = Q_e/A_e \tag{3}$$

$$\Delta t = t_w - (t_v + t_0)/2 \tag{4}$$

where q_e is heat flux, Q_e is heat load. A_e is the total surface area of the inner wall of the evaporator section. t_w is the mean wall temperature of the evaporator section. t_v is the operating temperature of the CPL evaporator. t_0 is the temperatures of working fluid at evaporator inlet. The t_0 introduced in the calculation of heat transfer coefficient is based on the following consideration: the temperatures of working fluid at evaporator inlet are slightly different for all experiment even though other experiment conditions are same.

Fig. 5 shows the heat transfer coefficient with respect to different charging rate for different heat load and reservoir temperature. The heat load is 20 W and 25 W when the reservoir temperature is 40 °C and 60 °C, respectively. From Fig. 5, it is found that the heat transfer coefficients increase firstly and then decrease as the charging rate increases. At the heat load 20 W, reservoir temperature 40 °C, the tendency reverses when the charging rate increases over 76%. Moreover, it presented very fast decrease for heat transfer coefficient with charging rate. This is probably due to inadequate liquid charging of the evaporator. At higher charging rate, the overcharge liquid may prevent the vapor from leaving rapidly to the evaporator and result in an increase in the temperature of the evaporator. The similar case also occurs at the heat load 25 W, reservoir temperature 60 °C. Therefore, a conclusion can be drawn from above results that there are the maximum values of

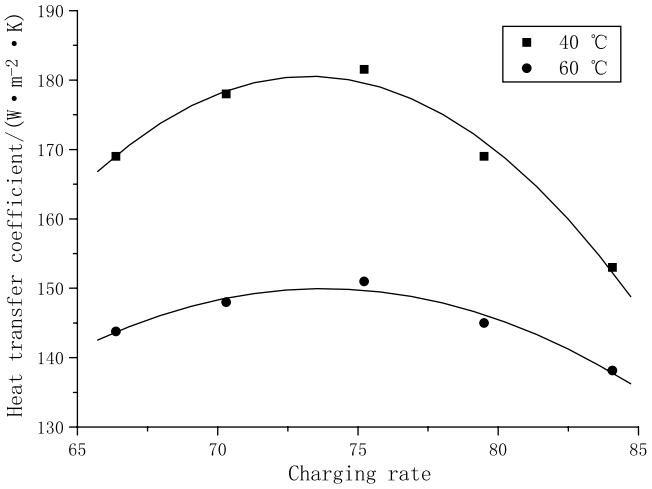

Fig. 5. Effects of charging rate on heat transfer performance of the evaporator.

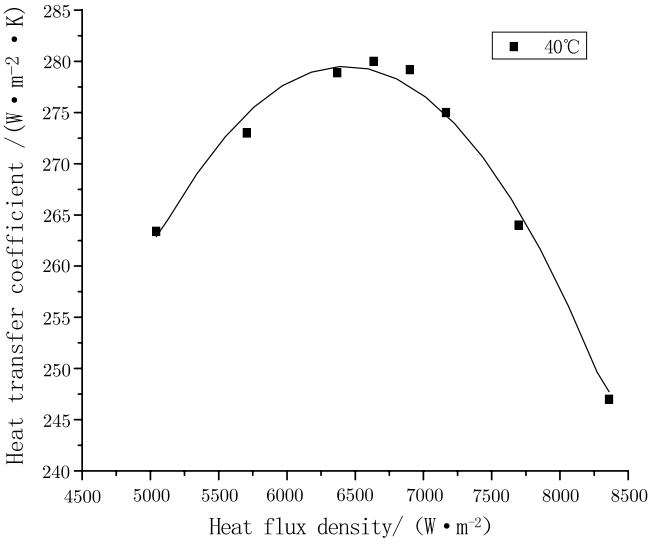

Fig. 6. Effects of heat flux density on heat transfer performance of the evaporator.

heat transfer coefficients corresponding to each heat load and reservoir temperature. According to the results, there may exist an optimal charging rate within the range of 70–76%.

Fig. 6 shows the experimental results of the average heat transfer coefficient with respect to different heat flux when the charging rate is 75% and the reservoir temperature is 40 °C. It is also seen that the heat transfer coefficients increase firstly and then decrease as the heat flux increases. There is the maximum value of heat transfer coefficients corresponding to a heat flux. This case may be explained as that when the heat flux is at lower the evaporation of liquid in the capillary wick could be achieved adequately, which cause the mass flow rate increase with increasing the heat flux. However, with the further increase in the heat flux, the small bubbles coalesced in the capillary wick forming vapor patches which insulated the heater block from the working fluid. These processes impede the liquid flow in the wick and the evaporation zone of liquid would dry out gradually, and thus limits the heat transfer process. Although the heat can be removed from the evaporator, the durable dryout region extends and the average heat transfer coefficients decrease rapidly.

4. Conclusions

This paper describes a proposed capillary pumped loop using the multi-layer copper mesh as the capillary structure in the evaporator, which was designed to accomplish the heat recovery applications in the field of the refrigeration and air conditioning. Experimental tests regarding the startup and heat transfer performance of the CPL were performed. The tests presented good performance for both startup and continuous operation. The experimental results indicate that the charging rate and the heat flux have effects on heat transfer performance. The optimal charging rate was found within the range of 70–76% for the given experimental conditions. Also, there exists a maximum heat transfer coefficient when the charging rate and reservoir temperature are fixed.

References

[1] J. Ku, Overview of capillary pumped loop technology, in: ASME HTD-vol. 236, Heat Pipes and Capillary Pumped Loops, 1993, pp. 1–17.
[2] Yu.F. Maydanik, State-of-the-art of CPL and LHP technology, in: Heat Pipe Science and Technology, Proc. 11th Int. Heat Pipe Conference, Tokyo, 1999, pp. 19–30.
[3] I. Muraoka, F.M. Ramos, V.V. Vlassov, Experimental and theoretical investigation of a capillary pumped loop with a porous element in the condenser, Int. Commun. Heat Mass Transfer 25 (8) (1998) 1085–1094.
[4] E. Bazzo, M. Nogoseke, Capillary pumping systems for solar heating application, Appl. Therm. Eng. 23 (9) (2003) 1153–1165.
[5] T.J. LaClair, I. Mudawar, Thermal transients in a capillary evaporator prior to the initiation of boiling, Int. J. Heat Mass Transfer 43 (21) (2000) 3937–3952.
[6] P.C. Chen, W.K. Lin, The application of capillary pumped loop for cooling of electronic components, Appl. Therm. Eng. 21 (17) (2001) 1739–1754.
[7] E. Bazzo, R.R. Riehl, Operation characteristics of a small-scale capillary pumped loop, Appl. Therm. Eng. 23 (6) (2003) 687–705.
[8] E. Pouzet, J.L. Joly, V. Platel, J.-Y. Grandpeix, C. Butto, Dynamic response of a capillary pumped loop subjected to various heat load transients, Int. J. Heat Mass Transfer 47 (10–11) (2004) 2293–2316.